Automated Design of a Broadside-Radiating Linearly Polarized Isotropic Metasurface Antenna

Original
Automated Design of a Broadside-Radiating Linearly Polarized Isotropic Metasurface Antenna / Zucchi, M.; Scarabosio, A.; Righero, M.; Giordanengo, G.; Vernì, F.; Vecchi, G.. - ELETTRONICO. - (2023), pp. 1767-1768. (Intervento presentato al convegno 2023 IEEE International Symposium on Antennas and Propagation and USNC-URSI Radio Science Meeting (USNC-URSI) tenutosi a Portland, OR, USA nel 23-28 July 2023) [10.1109/USNC-URSI52151.2023.10237751].

Availability:
This version is available at: 11583/2982050 since: 2023-10-04T11:19:37Z

Publisher:
IEEE

Published
DOI:10.1109/USNC-URSI52151.2023.10237751

Automated Design of a Broadside-Radiating Linearly Polarized Isotropic Metasurface Antenna

M. Zucchi$^{(1)}$, A. Scarabosio$^{(2)}$, M. Righero$^{(2)}$, G. Giordanengo$^{(2)}$, F. Vernì$^{(3)}$, and G. Vecchi$^{(1)}$

$^{(1)}$ Department of Electronics and Telecommunications, Politecnico di Torino, Turin, Italy (marcello.zucchi@polito.it)
$^{(2)}$ Advanced Computing, Photonics & Electromagnetics (CPE), Fondazione LINKS, Turin, Italy
$^{(3)}$ Huawei, Milan Research Center, Segrate, Italy

Abstract—**We present the automated design of a broadside-radiating metasurface antenna. The design is carried out by employing a continuous isotropic Impedance Boundary Condition through an optimization procedure based on the equivalent surface current only. A modified gradient-descent optimization algorithm is applied to minimize an objective function that incorporates both realizability and far field requirements. The antenna is then implemented by a suitable arrangement of circular unit cells, selected from a database of precomputed shapes. This procedure is applied to the design of a broadside-radiating, linearly polarized circular metasurface antenna working at 23 GHz, with size $\approx 12\lambda$. The obtained design is then validated with commercial software simulations.**

I. INTRODUCTION

Metasurface antennas are a novel type of antennas typically made up of a thin layer of metamaterial engineered to have unique electromagnetic properties. These properties allow the metasurface to manipulate electromagnetic waves in a way that is not possible with traditional antennas [1]. They have the potential to be more efficient and more versatile than traditional antennas, making them a promising technology for a wide range of applications.

Metasurfaces are constituted by the arrangement of a large number of subwavelength scattering elements. As such, their design is characterized by a large number of degrees of freedom, making a direct design not feasible in most practical cases. The design is tackled by modelling the metasurface as a layer of Impedance Boundary Condition (IBC), which allows for efficient algorithms to be exploited for the electromagnetic analysis. The implementation of the IBC layer is then based on the arrangement of small scatterers, properly shaped to produce the desired value of impedance locally.

Different methods have been proposed for the IBC design: some relying on analytical approximations [2], while other based on numerical approaches [3]. The current-based method presented by the authors in [4], applicable to isotropic metasurfaces only, has the advantage of not requiring any a priori knowledge on the impedance profile (a reduced order parameterization is not needed) making it particularly suited for cases in which the profile is not known analytically, e.g., shaped beams.

To verify the capabilities of the above mentioned method, it is applied to the case of a linearly polarized broadside beam antenna, which is known to be challenging to design with isotropic metasurfaces (in contrast to circular polarization). The obtained IBC profile is then implemented with circular patches, and the final design is then validated with full-wave simulations.

II. SYNTHESIS OF METASURFACE ANTENNAS

A. IBC Synthesis

The behaviour of a metasurface can be modeled macroscopically by means of a locally-varying scalar Impedance Boundary Condition (IBC), a linear relationship between the tangential electric field and the equivalent surface current, i.e., $\boldsymbol{E}_{\mathrm{t}} = Z_{\mathrm{s}} \boldsymbol{J}_{\mathrm{s}}$. Impedance values are constrained to be reactive in the case of lossless scatterers, $Z_{\mathrm{s}} = \mathrm{j} X_{\mathrm{s}}$.

The IBC synthesis is carried out with the current-based algorithm introduced in [4]. To this aim, the radiating surface is discretized with a triangular mesh, and the current is expanded as a linear combination of Rao-Wilton-Glisson (RWG) basis functions. The problem is formulated as the unconstrained minimization of a non-convex objective function that incorporates both realizability and radiation constraints, and the resulting output is in the form of an optimized current. This technique utilizes fast routines for electromagnetic analysis to evaluate gradients and employs a global polynomial strategy for line-search, enabling the design of large antennas.

The impedance is then obtained from the optimal current and the corresponding electric field with a local matching process. The algorithm is capable of treating open circuit conditions (absence of metasurface), a feature that is missing from most of the previously proposed approaches, enhancing the solution space.

B. Unit-cell database

The implementation of the metasurface from the optimized impedance profile relies on a precomputed database of unit cell shapes. For each shape, a simulation is carried out with a periodic approximation (which models the coupling between neighbouring cells) and the impedance value is extracted following the method presented in [5].

For the isotropic impedance case, the considered cells are *circular patches* with varying radius. The unit cell has a side length of $L = \lambda/6 = 2.2$ mm and the radius varies from $0.5L$ to $0.9L$ for a total number of 1000 different shapes. The covered reactance range is from $-1500\,\Omega$ to $-100\,\Omega$

III. RESULTS

The algorithm was applied to design a circular metasurface antenna working at 23 GHz. The diameter is $D =$

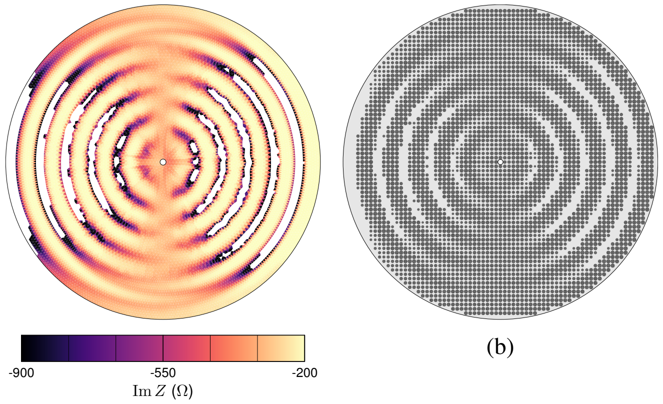

(a)

(b)

Fig. 1: Circular MTS antenna with linear pol. broadside radiation: (a) Optimized continuous impedance profile, (b) implementation with circular unit-cells.

158 mm $\approx$ 12 λ, placed on a grounded dielectric slab with $\varepsilon_{\mathrm{r}} = 3.34$ and thickness $h = 0.508$ mm. The antenna is fed through a vertical pin, which excites a surface wave on the dielectric. The height of the pin is optimized to maximize input matching in absence of the metasurface. The surface was discretized with 32 472 RWG basis functions.

Pattern constraints included a 10° HPBW in the broadside direction, linear polarization along the x-axis, with cross-polarization and sidelobes levels below -25 dB. The surface reactance was constrained between $-1000\,\Omega$ and $-200\,\Omega$.

Fig. 1a and Fig. 1b show the optimized IBC profile and its associated implementation. The impedance profile is clearly symmetric, as expected from the symmetry of the radiation constraints, and resembles previously published analytical profiles for linear polarization [6], [7], even though the optimization algorithm did not incorporate any a priori information.

The final design has been simulated with an in-house frequency domain MoM solver, as well as with the time domain solver in CST. The resulting directivity pattern is shown in Fig. 2, together with the design constraint. The co-polarization component complies with the requirements, with a maximum directivity of 22.5 dB (15% aperture efficiency), while the cross-polarization did not completely meet the constraints. This can be motivated by the limited flexibility offered by isotropic unit cells, and can be significantly improved by using anisotropic ones. The computed input reflection coefficient is $S_{11} = -19.4$ dB.

IV. CONCLUSIONS

The presented work provides evidence for the efficacy of current-based automated design applied to metasurface antennas. The design of a circular metasurface antenna with broadside radiation and linear polarization has been validated with full-wave simulations. Difficulty in meeting the radiation criteria for the cross-polarization component can be attributed to the use of isotropic impedance.

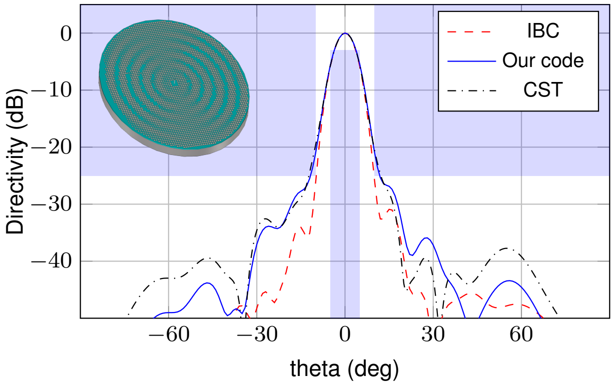

(a) Co-polarization

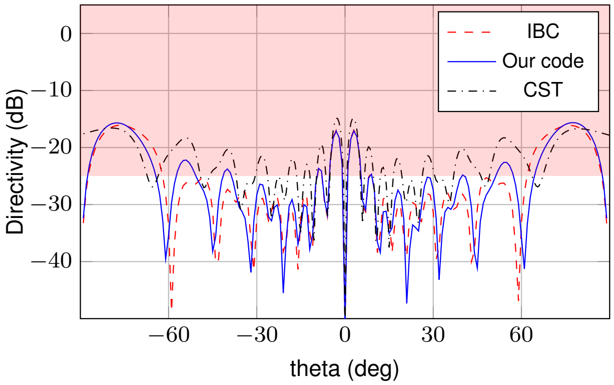

(b) Cross-polarization

Fig. 2: Normalized directivity in the plane cut $\varphi = 90°$: (a) co-polarization and (b) cross-polarization. “IBC” refers to the pattern obtained with a continuous impedance profile.

ACKNOWLEDGEMENT

This work was supported by the Italian Ministry of Research project PRIN 2020EY2LJT “METEOR”.

REFERENCES

[1] M. Faenzi, G. Minatti, D. González-Ovejero, F. Caminita, E. Martini, C. D. Giovampaola, and S. Maci, “Metasurface Antennas: New Models, Applications and Realizations,” *Sci Rep*, vol. 9, no. 1, pp. 1–14, Jul. 2019.

[2] G. Minatti, F. Caminita, M. Casaletti, and S. Maci, “Spiral Leaky-Wave Antennas Based on Modulated Surface Impedance,” *IEEE Trans. Antennas Propag.*, vol. 59, no. 12, pp. 4436–4444, Dec. 2011.

[3] M. Bodehou, C. Craeye, and I. Huynen, “Electric Field Integral Equation-Based Synthesis of Elliptical-Domain Metasurface Antennas,” *IEEE Trans. Antennas Propag.*, vol. 67, no. 2, pp. 1270–1274, Feb. 2019.

[4] M. Zucchi, F. Vernì, M. Righero, and G. Vecchi, “Current-Based Automated Design of Realizable Metasurface Antennas with Arbitrary Pattern Constraints,” Aug. 2022.

[5] A. M. Patel and A. Grbic, “Modeling and Analysis of Printed-Circuit Tensor Impedance Surfaces,” *IEEE Trans. Antennas Propag.*, vol. 61, no. 1, pp. 211–220, Jan. 2013.

[6] A. Arroyo, R. Contreres, A. Piche, H. Roussel, and M. Casaletti, “Linear Polarization from Scalar Modulated Metasurfaces,” in *2022 16th Eur. Conf. Antennas Propag. EuCAP*, Mar. 2022, pp. 1–4.

[7] D. González-Ovejero, N. Chahat, R. Sauleau, G. Chattopadhyay, S. Maci, and M. Ettorre, “Additive Manufactured Metal-Only Modulated Metasurface Antennas,” *IEEE Trans. Antennas Propag.*, vol. 66, no. 11, pp. 6106–6114, Nov. 2018.